Published in final edited form as:
Nature. 2007 May 17; 447(7142): 321–325. doi:10.1038/nature05736.

SUMOylation regulates kainate-receptor-mediated synaptic transmission

Stéphane Martin[1], **Atsushi Nishimune**[1], **Jack R. Mellor**[1], and **Jeremy M. Henley**[1]
[1]MRC Centre for Synaptic Plasticity, Anatomy Department, University Walk, University of Bristol, Bristol, BS8 1TD, UK

Abstract

The small ubiqwitin-like modifier protein (SUMO) regulates transcriptional activity and the translocation of proteins across the nuclear membrane[1]. The identification of SUMO substrates outside the nucleus is progressing[2] but little is yet known about the wider cellular role of protein SUMOylation. Here we report that in rat hippocampal neurons multiple SUMOylation targets are present at synapses and we show that the kainate receptor subunit GluR6 is a SUMO substrate. SUMOylation of GluR6 regulates endocytosis of the kainate receptor and modifies synaptic transmission. GluR6 exhibits low levels of SUMOylation under resting conditions and is rapidly SUMOylated in response to a kainate but not an *N*-methyl-D-aspartate (NMDA) treatment. Reducing GluR6 SUMOylation using the SUMO-specific isopeptidase SENP-1 prevents kainate-evoked endocytosis of the kainate receptor. Furthermore, a mutated non-SUMOylatable form of GluR6 is not endocytosed in response to kainate in COS-7 cells. Consistent with this, electrophysiological recordings in hippocampal slices demonstrate that kainate-receptor-mediated excitatory postsynaptic currents are decreased by SUMOylation and enhanced by deSUMOylation. These data reveal a previously unsuspected role for SUMO in the regulation of synaptic function.

Kainate receptors (KARs) have key roles in the regulation of synaptic transmission and neuronal excitability in the mammalian brain. At the presynaptic terminal they can modulate neurotransmitter release, and at the postsynaptic membrane they contribute to fast excitatory synaptic transmission[3]. The GluR6 subunit is expressed throughout the brain but is particularly abundant in the hippocampus, where GluR6 subunits can be present in both pre- and post-synaptic KAR complexes[4].

We identified the specific SUMO-conjugating enzyme Ubc9 and the SUMO ligase PIAS3 (Supplementary Figs 1, 2) as GluR6a interactors in a yeast two-hybrid screen. Of the ionotropic glutamate receptor subunits tested, only GluR6a exhibited strong interaction with both enzymes (Fig. 1a). These interactions were verified by co-immunoprecipitation of Ubc9 and PIAS3 with an anti-GluR6 antibody (Supplementary Fig. 1b, c). Truncation

Author Contributions S.M. and A. N. are co-first authors; J.R.M. and J.M.H. are co-last authors. S.M. performed surface expression, biochemistry and cell imaging assays in cell culture. A.N. made the original observation that GluR6a is a SUMOylation substrate, performed biochemistry on brain extracts and performed all molecular biological experiments. J.R.M. performed the electrophysiology experiments and co-wrote the manuscript. J.M.H. provided team leadership, project management and wrote the manuscript. All authors contributed to hypothesis development, experimental design and data interpretation.

Author Information Reprints and permissions information is available at www.nature.com/reprints. The authors declare no competing financial interests. Correspondence and requests for materials should be addressed to J.M.H. (j.m.henley@bris.ac.uk).

Supplementary Information is linked to the online version of the paper at www.nature.com/nature.

Full Methods and any associated references are available in the online version of the paper at www.nature.com/nature.

Europe PMC Funders Author Manuscripts

mutagenesis mapped the GluR6 interaction domain (Fig. 1b) to residues 882–895 which, alone among the KAR subunits, contains the consensus SUMOylation motif ΨKXE (ref. 5).

We next probed subcellular fractions with specific anti-SUMO-1 antibodies (Fig. 1c, Supplementary Figs 3, 5). Multiple SUMO-conjugated proteins were detected in all fractions, including high levels in the synaptosomal and postsynaptic density fractions (Fig. 1c). SUMOylation is readily reversible[6], so we assessed the effects of the cysteine isopeptidase inhibitor *N*-ethylmaleimide (NEM)[7]. Detection of SUMOylated proteins was markedly reduced in the absence of NEM (Supplementary Fig. 3a). Furthermore, in brain extracts a distinct higher-molecular-mass GluR6 band was detected in the presence of NEM (Fig. 1d). A specific GluR6 band was also detected in anti-SUMO antibody immunoprecipitates from cultures (Fig. 1e, Supplementary Fig. 5a) further confirming that GluR6 is SUMOylated in hippocampal neurons. As a control, the known SUMO substrate RanGAP1 was also retrieved in SUMO immunoprecipitates (Supplementary Fig. 4a, c). Interestingly, however, SUMOylated surface-expressed GluR6 was not detected in resting cultured neurons (Fig. 1e). Consistent with the yeast two-hybrid data, no corresponding band shift in the presence of NEM was observed for the AMPA receptor subunit GluR1 (Fig. 1e, Supplementary Fig. 4b).

As expected, we found high levels of SUMO immunoreactivity in the nucleus of cultured neurons. SUMO immunoreactivity was also distributed throughout dendrites (Fig. 1f–h), where it displayed a punctate distribution similar to those of GluR6, Ubc9 and PIAS3 (Supplementary Fig. 1d, e) and was present at PSD95-positive synapses (Supplementary Fig. 2a, b). Under basal conditions there were low levels of colocalization of surface-expressed GluR6 and SUMO-1 (5.3±0.8%) but there was some limited overlap between total GluR6 and SUMO-1 immunoreactivity (28.6±1.5%; Fig. 1f–h), indicating that most SUMOylated GluR6 is intracellular. The low level of colocalization between surface GluR6 and SUMO-1 is consistent with only a small fraction of substrate being SUMOylated at any given time[6,8].

Application of kainate or NMDA evokes internalization of GluR6 into distinct sorting pathways[9]. We therefore tested the effects of these agonists on GluR6 SUMOylation in immunoprecipitation experiments. Kainate (10 μM) rapidly increased the low basal level of GluR6 SUMOylation (Fig. 2a, b). This was detectable after 1 min (data not shown), increased >2-fold (2.4±0.4, $P<0.001$) at 3 min and reached maximal conjugation within 10 min (3.4±0.4, $P<0.001$). Glutamate (1 mM) also had similar effects (Supplementary Fig. 6). Despite strong NMDA-evoked internalization[9] there was no increase in GluR6 SUMOylation (Fig. 2a, b). Neither kainate nor NMDA altered global cellular SUMOylation (Supplementary Fig. 7). Similarly, in immunocytochemical assays colocalization between SUMO-1 and internalized GluR6 was 46.7±3.0% at 3 min and 54.1±4.9% at 30 min after adding kainate but only 15.9±1.8% at 3 min and 16.7±1.7% at 30 min after adding NMDA (Fig. 2c–h).

To explore the role of SUMOylation in agonist-evoked GluR6 endocytosis we expressed green fluorescent protein (GFP)-tagged SUMO specific isopeptidase SENP-1 (ref. 10) to facilitate deSUMOylation or its inactive point mutant SENP-1 C603S (ref. 11) (Supplementary Fig. 8). SENP-1, but not SENP-1 C603S, prevented kainate-evoked GluR6 internalization but had no effect on NMDA-evoked GluR6 internalization (Fig. 3a, b). Thus, GluR6 SUMOylation is required for kainate-evoked internalization and probably occurs at the plasma membrane. Because we did not detect SUMOylated GluR6 at the surface (Fig. 1e) we reasoned that internalization occurs rapidly after SUMOylation. Consistent with this, we detected surface-SUMOylated GluR6 in the presence of sucrose that blocks KAR endocytosis (Supplementary Fig. 9).

We next made glutathione *S*-transferase (GST) fusions of wild-type (WT) and K886R GluR6a carboxy-terminal domains for expression in a bacterial SUMOylation assay[12] to determine whether K886 within the consensus SUMOylation motif on GluR6a is the site of SUMOylation. Wild-type, but not K886R, C-terminal GluR6a was robustly SUMOylated (Fig. 3c). To evaluate the role of K886 SUMOylation in KAR endocytosis we compared the properties of the wild-type and K886R-tagged GluR6a tagged with yellow fluorescent protein (YFP). Both wild-type and K886R YFP–GluR6a display similar functional channel properties in COS-7 cells (data not shown). Wild-type YFP–GluR6a was surface-expressed in African green monkey kidney (COS-7) cells with minimal colocalization with SUMO-1 in unstimulated cells (Fig. 3d). Kainate caused a dramatic loss of surface YFP–GluR6a and strong colocalization with SUMO-1 in perimembrane compartments (Fig. 3e). YFP–GluR6a-K886R also trafficked to the plasma membrane (Fig. 3f) but its distribution was unchanged by kainate (Fig. 3f, g). The requirement of K886 for kainate-evoked internalization was further confirmed by surface biotinylation (Fig. 3h, i) and antibody feeding experiments (Supplementary Fig. 10). Kainate evoked massive endocytosis of wild-type YFP–GluR6a (72.9±1.8% at 30 min) but YFP–GluR6a-K886R internalization remained the same as constitutive endocytosis under non-stimulated conditions (12.4±0.6% compared to 11.3±0.9% in the presence of kainate at 30 min).

To identify a physiological role for GluR6 SUMOylation we investigated postsynaptic KARs at the mossy fibre synapse[13-15]. Under basal conditions stable, pharmacologically isolated, KAR-mediated, synaptically evoked excitatory postsynaptic currents (KAR-EPSCs) were recorded from CA3 neurons in hippocampal slices (Fig. 4a). Infusion of SUMO-1 into the CA3 neuron caused a rapid reduction in KAR-EPSC amplitude (97±5% and 77±8%; control versus SUMO-1; $P<0.05$). The conjugation-inactive mutant SUMO-1-ΔGG had no effect (100±6% and 77±6%; SUMO-1-ΔGG versus SUMO-1; $P<0.05$) (Fig. 4a, b, g). Infusion of recombinant SENP-1 increased the KAR-EPSC (98±11% and 145±13%; control versus SENP-1; $P<0.05$). Infusion of the inactive SENP-1 C603S mutant had no effect (91±11% and 145±21%; SENP-1 C603S versus SENP-1; $P<0.05$) (Fig. 4c, d, g). AMPA-receptor-mediated EPSCs recorded at the same synapse were unaffected by SUMO-1 or SENP-1 (89±9% and 101±13%; control versus SUMO-1; 101±18% and 91±13%; control versus SENP-1; Fig. 4e–g) or at CA1 Schaffer collateral synapses (Supplementary Fig. 11). KAR-EPSC decay kinetics were also unchanged by SUMO-1 (τ=30.3±2.1 ms during first 2 min of recording and 28.9±1.7 ms during last 5 min, n=11) or SENP-1 (τ=26.8±2.1 ms during first 2 min of recording and 25.6± 1.6ms during last 5 min, n=11).

We also infused SUMO-1 for 10 min before synaptic stimulation to determine whether SUMO-1 conjugation alone is sufficient to induce a decrease in KAR-EPSC amplitude. After the 10 min delay the reduction in KAR-EPSC amplitude was similar to those recorded immediately after membrane rupture (Fig. 4h), indicating that this process is activity-dependent because both SUMO-1 and agonist binding are required for the EPSC depression.

Our data indicate that the coincident action of agonist binding and SUMOylation to surface GluR6a leads to the rapid endocytosis of KARs. The observation that SENP-1 causes an increase in KAR-EPSC amplitude implies that when the removal of KARs is inhibited there is exocytosis and lateral diffusion of KARs into the synapse, as shown for AMPA receptors[16,17]. Also, NMDA stimulated GluR6 endocytosis is SUMO-1 independent, so there must be multiple KAR endo- and exocytosis pathways.

SUMO-1 regulation of KARs may be important in regulating the response of neurons to glutamate release under conditions such as ischaemia. Interestingly, it has been shown that SUMO-1 messenger RNA levels are dramatically raised in ischaemic cells[18]. Because

Europe PMC Funders Author Manuscripts

GluR6 is chronically downregulated by excitotoxic stress via a c-fos dependent mechanism[19], one attractive possibility is that upregulation of SUMO levels leads to a downregulation in KARs, thereby reducing neuronal excitability. The mechanisms by which SUMOylation of GluR6 leads to internalization are unclear, but it seems likely that regulation of interacting proteins[20,21] may be involved.

Our findings, taken together with the diverse range of functions that SUMO serves in the nucleus and cytoplasm, suggest that this covalent protein modification is likely to regulate the functions of many different synaptic proteins. We anticipate that synaptic SUMOylation represents a novel mechanism that will have far-reaching implications for understanding synaptic function.

METHODS SUMMARY

Yeast two-hybrid screen

Rat GluR6a C-terminal (841E–908A) domain was used as a bait to screen the rat whole-brain complementary DNA library.

Dissociated hippocampal cultures

Hippocampal cultures were prepared as previously reported[20] and plated at a density of 500,000 per 60 mm dish or 50,000 onto 22 mm glass coverslips coated with poly-L-lysine.

Biotinylation of cell surface protein

Live hippocampal neurons(21–25 days *in vitro*) were surface biotinylated on ice using the membrane impermeant Sulfo-NHS-SS-biotin.

Fluorescence imaging of GluR6

Live cultured hippocampal neurons (21–25 days *in vitro*) were transduced with Sinbdis to express appropriate protein constructs. Immunocytochemical imaging of surface and internalized receptors was performed on live and fixed cells using a Zeiss Meta confocal microscope.

Electrophysiology

Hippocampal slices were prepared from p14 Wistar rats. Whole-cell patch clamp recordings were made from visually identified CA3 pyramidal neurons and synaptic responses were recorded within 30 s of entering the whole-cell configuration.

Supplementary Material

Refer to Web version on PubMed Central for supplementary material.

Acknowledgments

We acknowledge the Wellcome Trust (J.M.H.), the MRC (J.R.M. and J.M.H.) and the EU (J.M.H. from a GRIPPANT contract) for financial support. We thank G. Hodgkinson for validation electrophysiology experiments on recombinant GluR6 in HEK cells, and S. Correa for some preliminary immuno cytochemistry experiments. We also thank M. Fleck for anti-GluR6 antibody, S. Goldstein for the SENP-1 constructs, C. Mulle for the pcDNA3-myc-GluR6 and H. Saitoh for the bacterial SUMOylation system. We are grateful to M. Ashby, G. Banting, Z. Bashir, T. Bouschet, G. Collingridge, J. Hanley, J. Isaac, F. Jaskolski, A. Randall and D. Stephens for commenting on the manuscript.

APPENDIX

METHODS

Plasmids

A full list of the plasmids used in this study is provided in the Supplementary Notes under 'Plasmids'. Rat GluR6 C-terminal domain (accession number NM_019309) was subcloned into pBTM116. Truncation series were prepared by polymerase chain reaction (PCR). Human SUMO-1 (accession number NM_003352) was amplified from a brain cDNA library (Invitrogen). The His6–SUMO-1 fragment was produced by amplifying with a forward primer containing a *Bam*HI site before the start codon and a reverse primer inserting a stop codon followed by a *Xho*I site. Amplified fragments were digested and inserted into the pET30a(+) (Novagen) vector. pET30-His6–S-tag–SUMO-1–GST was prepared by inserting the full-length GST fragment amplified from pGEX4T-1 (Amersham Biosciences) after removing the stop codon from pET30-SUMO-1. The pMax(+)-SENP-1 (accession number BC045639) (both wild-type and C603S mutant) was a gift from S. Goldstein. GST–SENP-1-wild-type and GST–SENP-1-C603S were constructed by inserting SENP-1 between the *Bam*HI and *Sal*I sites in pGEX4T-1. The SENP-1 fragment, containing an entire isopeptidase catalytic domain, was excised as a *Xho*I and *Eco*RI fragment and inserted into pEGFP-C1 (Clontech) vector. GFP–SENP fusion constructs were then excised from pEGFP–SENP-1-wild-type/C603S between *Nhe*I and *Bsp*120I and inserted into the *Xba*I and *Bsp*120I site of pSinRep5(nsP2Ser) vector. Site-directed mutagenesis was performed using the QuickChange II or QuickChange II XL (Stratagene) systems according to the manufacturer's protocol. The integrity of all cDNA constructs was verified by DNA sequencing. To prepare the plasmid pcDNA3.2-YFP–myc6–GluR6 (wild-type and K886R) constructs, YFP–myc6–GluR6 (wild-type) was made by inserting the YFP fragment into the *Cla*I site at the 5′ side of the myc6 tag of pcDNA3-myc-GluR6 (gift from C. Mulle). After a new *Not*I site was created at the 3′ side of the stop codon by site-directed mutagenesis, 3′-UTR was removed as a *Not*I–*Not*I fragment. The K886R mutation was introduced by site-directed mutagenesis. The *Asp*718I-*Not*I insert fragment was subcloned into the same sites of the entry plasmid pENTR1A (Invitrogen). The expression plasmids were generated from site-specific recombination between these entry plasmids and pcDNA3.2/V5-DEST (Invitrogen) by using LR Clonase (Invitrogen) site-specific recombinase according to the manufacturer's protocol.

Yeast two-hybrid screen

L40 yeast strain bearing the C-terminal GluR6 bait plasmid pBTM116-GluR6(841–908) were transformed with the oligo-dT and random hexamer-primed rat whole-brain pGAD10 cDNA library (Clontech). Yeast colonies that grew in less than 4 days at 30 °C under selective conditions were streaked on SD-Trp-Leu-His and subjected to the β-galactosidase assay. Screens were performed as described previously[22]. Briefly, library plasmids containing rat-brain cDNAs were rescued from yeast and into *E. coli* strain HB 101, which contains the leuB mutation. Transformants were selected by ampicillin resistance and leucine autotrophy. Rescued plasmids were digested with *Eco*RI and classified according to their restriction patterns. Each representative plasmid was re-transformed into both L40 bearing the pBTM-GluR6 and L40 bearing the control bait plasmid pBTM-LAM. Yeast were plated on SD-Trp-Leu-His and subjected to the filter β-galactosidase assays to confirm the reproducibility and specificity of the interactions. The identities of the rat cDNA encoding Ubc9 and PIAS3 were determined by sequencing using pGAD10 specific primer followed by BLAST (http://www.ncbi.nlm.nih.gov/BLAST/) analysis.

Virus preparation and transduction of hippocampal cultured neurons

Attenuated sindbis virus (SINrep(nsP2S726)) was prepared and used as previously reported[23]. cRNA was synthesized with an mMESSAGE mMACHINE SP6 kit after vector linearization (Ambion). cRNA from the construct in pSinRep5(nsP2S726) and the defective helper plasmid (pDH-BB(tRNA/TE12)) were mixed and electroporated into baby hamster kidney (BHK21) cells. 48 hours after electroporation, the culture medium containing the pseudovirions was harvested, ultracentrifuged and the pellet resuspended in a minimum volume of Neurobasal medium (Gibco). Aliquots of virus were stored at −80 °C. Cultured hippocampal neurons were transduced at a multiplicity of infection (MOI) of 3 and returned to the incubator for 24 to 48 h before use.

Expression and purification of recombinant proteins

pET-SUMO1(1–97; active form), pET-SUMO(1–95; ΔGG-conjugation-deficient form), or pET-His6–S-tag–SUMO1–GST were introduced to BL21(DE3) for recombinant protein expression. pGEX-SENP-1-wild-type and pGEX-SENP-1-C603S were introduced to BL21 for expression. Cells are cultured to the early-log phase and protein expression was induced by adding isopropyl-β-$_{D}$-thiogalactoside (IPTG) at 0.2 mM final concentration. Cells were harvested and lysed by sonication in 1% Triton X-100, 5 mg ml^{-1} lysozyme and 20 U ml^{-1} Benzonase (Novagen) containing PBS(−). Cleared lysate was prepared by centrifuged at 35,000*g* for 20 minutes at 4 °C. His6-tagged proteins were purified with TALON Co^{2+} affinity resin (Clontech) and GST fusion proteins were purified by using glutathione Sepharose 4B (Amersham Biosciences), according to the manufacturer's protocols. After affinity chromatography purification, eluates were extensively dialysed against PBS(−) and the buffer exchanged to the intracellular solution for patch pipette using NAP-5 Sephadex G-25 columns. Eluates were adjusted to 100× concentration stocks and stored at −80 °C until use.

SUMOylation assay in *E. coli*

The bacterial SUMOylation assay was performed as described previously[12].

In vitro assay of recombinant SENP

The recombinant SENP substrate His6–S-tag–SUMO1–GST was purified by Co^{2+} affinity chromatography. Assays were performed in 10 mM Tris-HCl (pH 7.5), 150 mM NaCl, and 1 mM dithiothreitol (DTT). Reactions were incubated for 2 h at 30 °C. Proteins were subjected to SDS–polyacrylamide gel electrophoresis (PAGE) and electrotransfer onto PVDF-membrane. After blocking, intact and cleaved bands were detected by HRP-conjugated S-protein (Novagen) and chemiluminescence substrate.

Preparation of brain fractions

Brains from adult Wistar rats (220 g) were rapidly removed and put into ice-cold phosphate-buffered saline (PBS). Whole brains were homogenized in 20 mM HEPES (pH 7.4) containing 0.32 M sucrose, 150 mM NaCl, 1 mM $MgCl_2$, 0.5 mM $CaCl_2$ and 20 mM NEM. Subcellular fractionations were obtained by differential centrifugation as previously described[24].

Dissociated hippocampal cultures

Hippocampal cultures were prepared using a modified published protocol[9]. Briefly, hippocampi from E18 Wistar rats were dissected and the neurons dissociated by enzymatic digestion with trypsin for 15 min and mechanical dissociation. Cells were then plated at a density of 500,000 per 35 mm dish or 50,000 onto 22 mm glass coverslips coated with poly-$_{L}$-lysine (Sigma). The culture medium was composed of Neurobasal medium (Gibco)

supplemented with horse serum (10%), B27 (Gibco) and 2 mM glutamine. On the second day, the media was changed to Neurobasal medium supplemented with B27 only and the neurons were then fed weekly with this glutamine-free medium until use (21–25 days *in vitro*).

Biotinylation of cell surface protein

Live hippocampal neurons (21–25 days *in vitro*) were surface biotinylated on ice using the membrane impermeant Sulfo-NHS-SS-Biotin (Pierce, 0.15 mg ml^{-1} in PBS). After three washes in TBS (Tris-HCl 25 mM, pH 7.4, NaCl 137 mM, KCl 5 mM, $CaCl_2$ 2.3 mM, $MgCl_2$ 0.5 mM, Na_2HPO_4 0.143 gl^{-1}) to quench the remaining free unbound biotin, the cells were lysed in extraction buffer (Tris-HCl 50 mM pH 7.5, NaCl 150 mM, EDTA 10 mM, Triton X-100 1%, SDS 0.1%, mammalian protease inhibitor cocktail 1% and NEM 20 mM). After sonication for 10 s and centrifugation (15,000*g* for 20 min at 4 °C) supernatants containing equal amount of protein were incubated with streptavidin beads to immunoprecipitate the surface-biotinylated proteins. After many washes in extraction buffer, proteins were eluted from the streptavidin beads by boiling in reducing sample buffer and then resolved by SDS-PAGE and immunoblotted using rabbit polyclonal antibodies against GluR1 (1/2,000, Upstate Biotechnology) and/or GluR6/7 (1/2,000, Upstate Biotechnology). Bands were quantified using ImageJ software (NIH) and normalized to the total receptor band intensity.

Internalization assay in COS-7 cells

Transiently transfected COS-7 cells were biotinylated as described above. After extensive washes, cells were subsequently incubated in the absence or in the presence of 100 μM kainate for the times indicated in the legend. The remaining surface biotin was removed with GSH buffer (pH 9, 2×20 min), then lysed and incubated with streptavidin beads to isolate internalized biotinylated proteins. After washing, proteins were eluted from the streptavidin beads, separated on SDS-PAGE and immunoblotted with anti-GluR6/7 antibody (1/2,000) as previously described[9].

Immunoprecipitation

200–400 μg of solubilized protein prepared as above was incubated with 2-4 μg of mouse monoclonal anti-SUMO-1 (D-11) antibody (from Santa Cruz) or 1/50 (v/v) rabbit anti-SUMO-1 (from Cell Signaling) overnight at 4 °C and then with 50 μl protein G-agarose beads (Sigma) for 1–3 h at 4 °C. Immunoprecipitates were washed four times with lysis buffer and proteins were eluted from the beads by boiling in reducing sample buffer and then resolved by SDS-PAGE.

Fluorescence imaging of GluR6 endocytosis

Live cultured hippocampal neurons (21–25 days *in vitro*) were transduced with sindbis virus containing the GFP-tagged catalytic domain of SENP-1 (active SENP-WT or its inactive form SENP-C603S) for 24 to 48 h. The neurons were then surface labelled for 20 min at room temperature with a chicken N-terminal directed anti-GluR6 antibody (1/4,000)[9,25,26]. Neurons were washed three times in PBS and then incubated for 30 min at 37 °C in Earle's-Tris-HEPES buffer containing 10 μM kainate (Tocris). For NMDA treatment, we used a modified protocol originally named "Chem-LTD"[27]. Briefly, neurons were stimulated at 37 °C with NMDA (30 μM) in Earle's-Tris-HEPES buffer for 3 min, and incubated in the same buffer in the absence of NMDA for the times indicated in the results. After a rapid 5 min fixation step in paraformaldehyde (4%), the remaining cell surface receptors were labelled with a Cy5-conjugated anti-chicken antibody (Jackson ImmunoResearch laboratories) for 45 min at room temperature. Neurons were then fixed for a further 15 min with

paraformaldehyde (4%), permeabilized for 2 min in PBS containing Triton X-100 (0.2%) and labelled with a Cy3-conjugated anti-chicken antibody (Jackson ImmunoResearch Laboratories) for one hour to visualize internalized receptors. Confocal images were acquired with a Zeiss LSM 510 confocal microscope and quantified using Volocity Software (Improvision). Values corresponding to the internalized receptors (red) were divided by the total fluorescence values (red + blue) to control for cell density and expressed as arbitrary units (a.u.).

COS-7 cells: YFP–myc6–GluR6a-WT and YFP–myc6–GluR6-K886R were transiently transfected in COS-7 cells and surface receptors were live labelled using an Alexa Fluor 647 coupled anti-GFP antibody for 10 min at room temperature (22 °C). After extensive washes in Earle's buffer at room temperature, cells were incubated at 37 °C for 20 min in Earle's buffer containing 100 μM kainate prior to fixation with paraformaldehyde (PAF) 4% in PBS for 5 min and labelling of remaining surface receptors with an Alexa Fluor 555 anti-GFP antibody. COS-7 cells were then washed in Earle's buffer and further fixed in PAF 4% in PBS for 15 min before mounting in Mowiol (Sigma) and confocal visualization.

Colocalization of internalized GluR6 with SUMO-1

Internalization experiments were carried out as above until the paraformaldehyde fixation, except that neurons were stimulated for 3 min with kainate (10 μM) and D-AP5 (50 μM) or NMDA (30 μM) for the indicated times at 37 °C. Remaining antibodies at the cell surface were removed by 2×2 min washes with low-pH Earle's buffer (0.5 M NaCl, pH 4 with acetic acid) and fixed for 20 min with paraformaldehyde (4%) as previously described[9]. After permeabilization, cells were incubated with anti-SUMO-1 (rabbit 1/100; Santa Cruz) and labelled with a Cy3-conjugated anti-chicken antibody to visualize internalized GluR6 and Cy2- or Cy5-conjugated secondary antibodies as indicated. Puncta corresponding to the internalized GluR6 that colocalized with the SUMO labelling were quantified using the LSM510 version 3.2 software (Zeiss). Analysis was made from at least eight cells for each condition.

Statistical analysis

Statistical analyses were performed using Prism 4 software (GraphPad). Data are expressed as mean±s.e.m. Unpaired Student's *t*-tests and one-way analysis of variance (ANOVA) were performed with a Newman-Keuls post-test for multiple comparison data sets when required.

Electrophysiology

Hippocampal slices were prepared from p14 Wistar rats as previously described[28]. For recording, slices were immersed in a submerged recording chamber perfused with solution containing 126 mM NaCl, 10 mM glucose, 26 mM $NaHCO_3$, 2.5 mM KCl, 1.2 mM $NaHPO_4$, 2.5 mM $CaCl_2$ and 1.3 mM $MgSO_4$ at 35 °C and saturated with 95% O_2, 5% CO_2. Whole-cell patch clamp recordings were made from visually identified CA3 pyramidal neurons using borosilicate glass pipettes of resistance 2–6 MΩ filled with a solution containing 117 mM $CsMeSO_4$, 8 mM NaCl, 10 mM HEPES, 5 mM QX-314Cl, 4 mM MgATP, 0.3 mM NaGTP, 0.2 mM EGTA, 0.1 mM bestatin and 0.1 mM leupeptin at pH 7.4 and 280 mOsm. Synaptic responses were recorded within 30 s of entering the whole-cell configuration and elicited using a bipolar tungsten electrode placed in the granule cell layer stimulated every 20 s with three pulses applied at 167 Hz. Kainate responses were recorded in 50 μM D-APV, 100 μM picrotoxin and 25–40 μM GYKI53655. For AMPA receptor recording, the concentration of $CaCl_2$ and $MgSO_4$ were raised to 4 mM each, GYKI53655 was omitted and stimulation was given as one pulse every 20 s. DCG-IV (2 μM) was applied at the end of 23 experiments, in each case depressing the EPSC by >80%.

References

22. Nishimune A, et al. NSF binding to GluR2 regulates synaptic transmission. Neuron. 1998; 21:87–97. [PubMed: 9697854]
23. Kim J, et al. Sindbis vector SINrep(nsP2S726): a tool for rapid heterologous expression with attenuated cytotoxicity in neurons. J. Neurosci. Methods. 2004; 133:81–90. [PubMed: 14757348]
24. Hirbec H, Martin S, Henley JM. Syntenin is involved in the developmental regulation of neuronal membrane architecture. Mol. Cell. Neurosci. 2005; 28:737–746. [PubMed: 15797720]
25. Fleck MW, Cornell E, Mah SJ. Amino-acid residues involved in glutamate receptor 6 kainate receptor gating and desensitization. J. Neurosci. 2003; 23:1219–1227. [PubMed: 12598610]
26. Mah SJ, Cornell E, Mitchell NA, Fleck MW. Glutamate receptor trafficking: endoplasmic reticulum quality control involves ligand binding and receptor function. J. Neurosci. 2005; 25:2215–2225. [PubMed: 15745947]
27. Lee HK, Kameyama K, Huganir RL, Bear MF. NMDA induces long-term synaptic depression and dephosphorylation of the GluR1 subunit of AMPA receptors in hippocampus. Neuron. 1998; 21:1151–1162. [PubMed: 9856470]
28. Daw MI, et al. PDZ proteins interacting with C-terminal GluR2/3 are involved in a PKC-dependent regulation of AMPA receptors at hippocampal synapses. Neuron. 2000; 28:873–886. [PubMed: 11163273]

References

1. Seeler JS, Dejean A. Nuclear and unclear functions of SUMO. Nature Rev. Mol. Cell Biol. 2003; 4:690–699. [PubMed: 14506472]
2. Wilson VG, Rosas-Acosta G. Wrestling with SUMO in a new arena. Sci. STKE. 2005; 2005:pe32. [PubMed: 15985640]
3. Lerma J. Roles and rules of kainate receptors in synaptic transmission. Nature Rev. Neurosci. 2003; 4:481–495. [PubMed: 12778120]
4. Jaskolski F, Coussen F, Mulle C. Subcellular localization and trafficking of kainate receptors. Trends Pharmacol. Sci. 2005; 26:20–26. [PubMed: 15629201]
5. Hilgarth RS, et al. Regulation and function of SUMO modification. J. Biol. Chem. 2004; 279:53899–53902. [PubMed: 15448161]
6. Johnson ES. Protein modification by SUMO. Annu. Rev. Biochem. 2004; 73:355–382. [PubMed: 15189146]
7. Suzuki T, et al. A new 30-kDa ubiquitin-related SUMO-1 hydrolase from bovine brain. J. Biol. Chem. 1999; 274:31131–31134. [PubMed: 10531301]
8. Hay RT. SUMO: a history of modification. Mol. Cell. 2005; 18:1–12. [PubMed: 15808504]
9. Martin S, Henley JM. Activity-dependent endocytic sorting of kainate receptors to recycling or degradation pathways. EMBO J. 2004; 23:4749–4759. [PubMed: 15549132]
10. Gong L, Millas S, Maul GG, Yeh ET. Differential regulation of sentrinized proteins by a novel sentrin-specific protease. J. Biol. Chem. 2000; 275:3355–3359. [PubMed: 10652325]
11. Rajan S, Plant LD, Rabin ML, Butler MH, Goldstein SA. Sumoylation silences the plasma membrane leak K1 channel K2P1. Cell. 2005; 121:37–47. [PubMed: 15820677]
12. Uchimura Y, Nakao M, Saitoh H. Generation of SUMO-1 modified proteins in E. coli: towards understanding the biochemistry/structural biology of the SUMO-1 pathway. FEBS Lett. 2004; 564:85–90. [PubMed: 15094046]
13. Vignes M, Collingridge GL. The synaptic activation of kainate receptors. Nature. 1997; 388:179–182. [PubMed: 9217158]
14. Castillo PE, Malenka RC, Nicoll RA. Kainate receptors mediate a slow postsynaptic current in hippocampal CA3 neurons. Nature. 1997; 388:182–188. [PubMed: 9217159]
15. Mulle C, et al. Altered synaptic physiology and reduced susceptibility to kainate-induced seizures in GluR6-deficient mice. Nature. 1998; 392:601–605. [PubMed: 9580260]
16. Luscher C, et al. Role of AMPA receptor cycling in synaptic transmission and plasticity. Neuron. 1999; 24:649–658. [PubMed: 10595516]

17. Borgdorff AJ, Choquet D. Regulation of AMPA receptor lateral movements. Nature. 2002; 417:649–653. [PubMed: 12050666]
18. Comerford KM, et al. Small ubiquitin-related modifier-1 modification mediates resolution of CREB-dependent responses to hypoxia. Proc. Natl Acad. Sci. USA. 2003; 100:986–991. [PubMed: 12552083]
19. Zhang J, et al. c-fos regulates neuronal excitability and survival. Nature Genet. 2002; 30:416–420. [PubMed: 11925568]
20. Hirbec H, et al. Rapid and differential regulation of AMPA and kainate receptors at hippocampal mossy fibre synapses by PICK1 and GRIP. Neuron. 2003; 37:625–638. [PubMed: 12597860]
21. Coussen F, et al. Co-assembly of two GluR6 kainate receptor splice variants within a functional protein complex. Neuron. 2005; 47:555–566. [PubMed: 16102538]

Europe PMC Funders Author Manuscripts

Europe PMC Funders Author Manuscripts

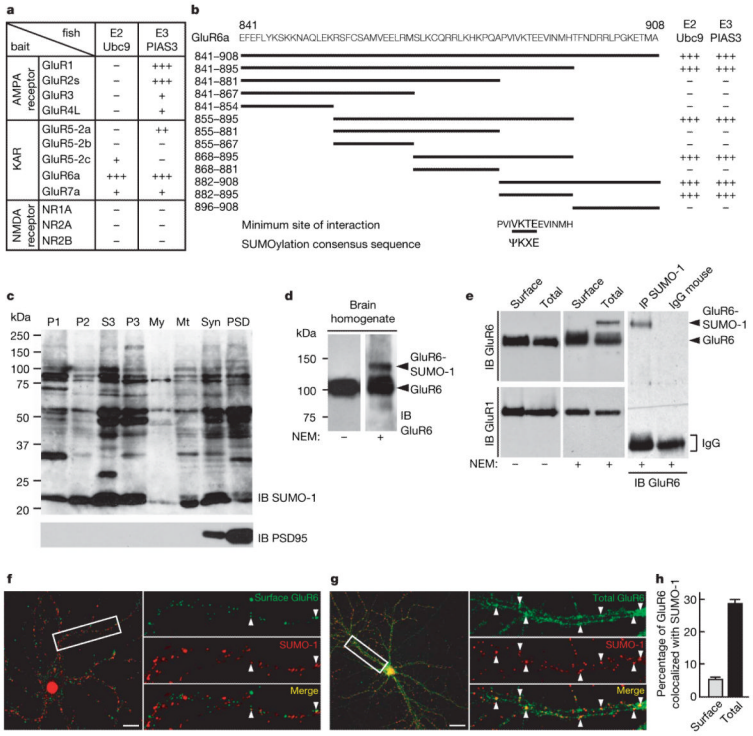

Figure 1. SUMOylation of GluR6 in brain and cultured hippocampal neurons

a, The SUMO-conjugating enzyme Ubc9 and the SUMO ligase PIAS3 selectively bind to the C-terminal domain of GluR6a in the yeast two-hybrid assay. The C termini of none of the other ionotropic glutamate receptor subunits tested interact strongly with both enzymes, as determined by β-galactosidase reporter activation. **b**, A series of overlapping truncation mutants of the C terminus of GluR6a tested in the yeast two-hybrid assay showed that the domain for both SUMOylation enzymes contains the consensus SUMOylation motif (ΨKXE, where Ψ is the hydrophobic residue). **c**, Immunoblot (IB) analysis of synaptic SUMOylated proteins after rat brain fractionation. Multiple SUMOylated substrates are present in the synaptic fractions. Equal amount of protein (40 μg protein per lane) from each fraction was loaded. P1, crude nuclear fraction; P2, post-nuclear crude membrane fraction; S3, cytosol; P3, microsomes; My, myelin; Mt, mitochondria; Syn, synaptosomes; PSD, post-synaptic density fraction. Immunoblot probed with anti-PSD95 antibody is shown below (2 μg protein per lane). We note that the PSD95 blot is loaded with very low levels of protein to avoid saturation of the signal in the highly enriched synaptic and postsynaptic density fraction lanes. **d**, Immunoblots showing SUMOylated and non-SUMOylated forms of GluR6a in brain homogenate. Note that, in the absence of the cysteine protease inhibitor NEM, no detectable band corresponding to SUMOylated GluR6a was observed, which confirms that the SUMO adduct is highly labile and sensitive to de-conjugation. **e**, Immunoblots showing SUMOylated and non-SUMOylated forms of GluR6a in cultured hippocampal neurons. Immunoprecipitation (IP) experiments using anti-SUMO-1 antibody reveal that a fraction of GluR6a is SUMOylated in cultured hippocampal neurons (right panel). IgG, immunoglobulin. The blots are representative of at least four separate experiments. **f**, **g**, Infrequent but punctate colocalization of surface (**f**) and total GluR6 (**g**) with total SUMO (in green) in unstimulated cultured hippocampal neurons. We note that SUMO is highly concentrated in the nuclear compartment, consistent with its described role in nuclear function, but also clearly show a punctate distribution along the dendrites. Arrowheads denote colocalization. Scale bar, 20 μm. **h**, Quantification of surface and total

GluR6 receptor population that colocalize with total SUMO-1 in unstimulated cultured hippocampal neurons as shown in **f** and **g**. Puncta corresponding to GluR6 that colocalized with the SUMO-1 labelling were quantified using the LSM510 version 3.2 software (Zeiss). Analysis was made from at least eight cells for each condition and given as a percentage ± s.e.m.

Europe PMC Funders Author Manuscripts

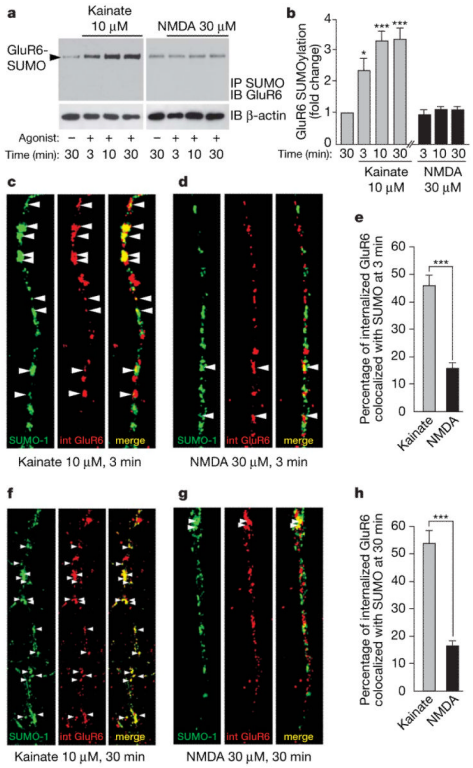

Figure 2. GluR6a is SUMOylated after direct stimulation with kainate in cultured hippocampal neurons

a, Immunoprecipitation of SUMOylated protein and immunoblotting for GluR6 shows that 10 μM kainate application dramatically increases GluR6 SUMOylation in a time-dependent manner. In contrast, 30 μM NMDA does not change the SUMOylation state of GluR6. Lower panels show an immunoblot of total β-actin as a control of protein loading. **b**, Quantification of kainate and NMDA-induced GluR6 SUMOylation shown in **a**. The data are from four separate experiments and show mean ± s.e.m. **P*<0.01 and ****P*<0.001 compared with unstimulated controls. **c**–**e**, Colocalization of SUMO-1 and endocytosed GluR6 3 min after 10 μM kainate (**c**) or 30 μM NMDA (**d**) stimulation. A significant proportion of internalized GluR6 (red) colocalizes as indicated by arrowheads (yellow) with SUMO-1 (green) after 3 min kainate stimulation, whereas few internalized ('int') receptors colocalize with SUMO-1 upon NMDA application, as quantified in **e**. Data show mean ± s.e.m. of three independent experiments. ****P*<0.0001 compared with NMDA stimulation (*t*-test). **f**–**h**, Colocalization of SUMO-1 and endocytosed GluR6 30 min after 10 μM kainate (**f**) or 30 μM NMDA (**g**) stimulation. A large proportion of GluR6 internalized (red) in response to kainate stimulation colocalizes (yellow; arrowheads) with the SUMO labelling (green) whereas few internalized receptors colocalize with SUMO when neurons are stimulated with NMDA. **h**, Quantification of the percentage of internalized GluR6 that colocalizes with SUMO-1 in response to either kainate or NMDA receptor activation. Data show mean ± s.e.m. of three independent experiments. ****P*<0.0001 compared with NMDA stimulation (*t*-test).

Europe PMC Funders Author Manuscripts

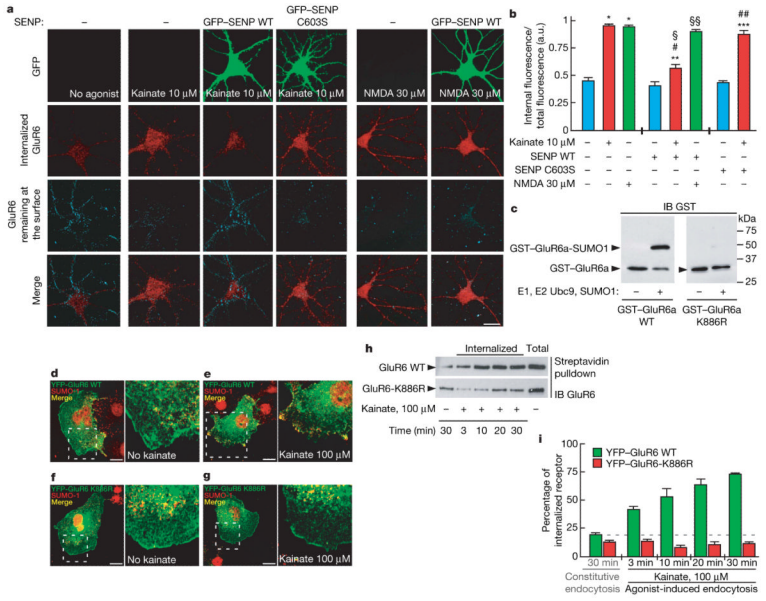

Figure 3. DeSUMOylation blocks kainate-induced GluR6 endocytosis

a, Effect of kainate (10 μM) and NMDA (30 μM) application for 30 min at 37 °C on the endocytosis of GluR6 assessed by immunofluorescence assays[9] (see Methods). Internalized GluR6 is shown in red and the remaining labelled surface receptors are visualized in blue. The green labelling represents the fluorescence due to the GFP expression from hippocampal neurons transduced for 24 h with sindbis virus expressing either the active form of SENP-1 (GFP-SENP-1-WT) or its inactive point mutant form (GFP-SENP-1-C603S). SENP-1 overexpression does not prevent GluR6 endocytosis induced by NMDA stimulation, indicating a specific involvement of the SUMOylation pathway in ligand-induced KAR endocytosis. Scale bar, 20 μm. **b**, Quantification of GluR6 endocytosis expressed in arbitrary units (a.u.) corresponding to the ratio between the internalized and total GluR6 labelling as shown in **a**. The data are from three separate experiments and show mean ± s.e.m. *$P < 0.001$ compared with untreated uninfected neurons; **$P < 0.01$ compared with untreated GFP-SENP-1-WT; ***$P < 0.001$ compared with untreated GFP–SENP-1-C603S; #$P < 0.001$ compared with kainate-stimulated uninfected neurons; §$P < 0.001$ compared with kainate-stimulated GFP-SENP-1-C603S; §§$P < 0.001$ compared with untreated GFP-SENP-1-WT; ##P<0.001 compared with untreated uninfected neurons. **c**, Bacterial SUMOylation assay. The C terminus of GluR6a but not GluR6a K886R is SUMOylated in a recombinant bacterial system (see Methods for details). **d**–**g**, YFP-tagged GluR6a wild-type (**d**, **e**) and GluR6a-K886R point mutant subunits (**e**, **f**) were transiently transfected in COS-7 cells and stained with anti-SUMO-1 antibody (red). Cells were exposed to 100 μM kainate at 37 °C for 10 min (**e**, **g**) to trigger endocytosis. Untreated control cells are shown in **d** and **f**. Right panels in **d**–**g** are enlargements of the hatched boxes in the left panels of **d**–**g**. Scale bar, 10 μm. **h**, Representative immunoblots showing the time course of YFP–GluR6a wild-type and YFP–GluR6a-K886R mutant receptor endocytosis following kainate stimulation. Experiments were performed on transiently transfected COS-7 cells using biotinylation assays (see Methods for details). i, Time course of kainate-induced GluR6a wild-type and K886R point-mutant receptor endocytosis measured by biotinylation assay from **h**. Each time point represents the mean ± s.e.m. of four independent experiments.

Europe PMC Funders Author Manuscripts

Europe PMC Funders Author Manuscripts

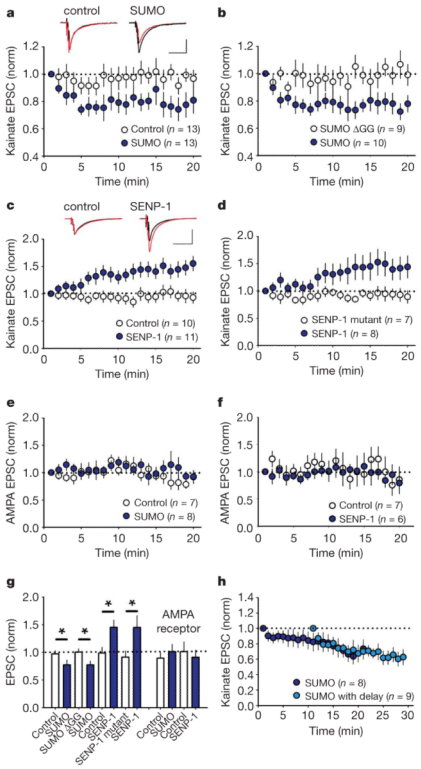

Figure 4. Synaptic KARs are regulated by SUMOylation

a, Inclusion of 4.2 μM active SUMO-1 protein into the patch pipette caused a significant rundown in the KAR-mediated EPSC compared to interleaved control experiments. Responses for each cell are normalized to the first minute after membrane rupture. Example traces are taken as the average from the first minute (black) and 15–20 min (red). Scale bars are 50 pA (vertical) and 100 ms (horizontal). **b**, Same as a but the control contains 4.2 μM of the conjugation-inactive mutant SUMO-ΔGG. **c**, Inclusion of 100 nM SENP-1 caused a significant increase in the EPSC compared to interleaved control experiments. Example traces are taken as the average from the first minute (black) and 15–20 min (red). Scale bars are 50 pA and 100 ms. **d**, Same as **c** but the internal control contains 100 nM of the inactive mutant SENP-1-C603S. e, AMPA-receptor-mediated EPSCs were unaffected by the inclusion of 4.2 μM active SUMO. **f**, AMPA receptor-mediated EPSCs were unaffected by the inclusion of 100 nM SENP-1. **g**, Quantification of results shown in **a**–**e**. Statistical significance denoted by * ($P < 0.05$, unpaired *t*-test). **h**, A 10 min delay in commencing synaptic stimulation caused a similar rundown in kainate EPSC to interleaved control experiments, where in both cases the pipette contained 4.2 μM active SUMO (69 ± 10% versus 61 ± 9% 15–20 min after start of stimulation). Norm, normalized. All error bars are means ± s.e.m.